

Analysis of the SPH Interpolation Moments Matrix with Regard to the Influences of the Discretization Error in Adaptive Simulations

Pascal Heinzelmann¹, Fabian Spreng^{2,3}, Daniel Sollich¹, Peter Eberhard¹, John R. Williams³

¹Institute of Engineering and Computational Mechanics, University of Stuttgart, Pfaffenwaldring 9, 70569 Stuttgart, Germany
pascal.heinzelmann@outlook.de; [daniel.sollich, peter.eberhard]@itm.uni-stuttgart.de

²ASESCO GmbH, Rainwiesen 41, 71686 Remseck am Neckar, Germany
f.spreng@asesco.de

³Department of Civil and Environmental Engineering, Massachusetts Institute of Technology, 77 Massachusetts Avenue, Cambridge, MA 02139, USA
[spreng, jrwl]@mit.edu

Abstract—The adaptive Smoothed Particle Hydrodynamics (SPH) method has great potential to reduce the computational demand of complex simulations by increasing the particle resolution in relevant areas and vice versa. The application of an adaptive SPH method requires a criterion which reliably identifies particles to be split or merged. The definition of a physical criterion is often not easy as it requires prior knowledge of the system to be investigated. This urges the need for a universal adaptivity criterion which is not dependent on the physical system’s properties. The so-called SPH interpolation moments matrix can be taken as a measure of the discretization accuracy actually achieved. It makes use of the zeroth- and first-order consistency conditions of the SPH interpolation and should be identical with the identity matrix of the given dimension. Deviations of this matrix from the ideal form may result from (i) an insufficient spatial resolution of the model domain, (ii) a non-uniformity of the neighboring particles’ distribution, and (iii) a truncated kernel-support at free surfaces. Up to now, there is no strategy allowing to distinguish between the influences on the matrix following from the different error sources. To deduce such a strategy, the structure of the matrix is thoroughly analyzed and its changes due to the three named influences were determined with the help of randomly generated and homogeneously distributed grids and a bursting dam example using the software Pasimodo.

I. INTRODUCTION

At the 10th International SPHERIC Workshop 2015, as part of the proceedings paper [1], a discretization-error-based refinement and coarsening criterion was introduced. The aim of this criterion is to identify areas to be refined or coarsened during the runtime of an SPH simulation and to apply particle refinement or coarsening strategies with the help of this information. Until now, such strategies require apriori knowledge of the simulated system or parallel calculations with different resolutions. A further contribution was made in [2] which led to an attempt to develop an adaptivity criterion for the efficient regulation of the dynamic resolution. This adaptivity criterion was further developed and applied to an example leading to good results [3].

The aim of this work is to analyze the SPH interpolation moments matrix which is used for the identification of areas to be refined or coarse. The analysis should lead to an improved adaptivity criterion and a minimization of the calculation effort.

In the following, a brief introduction to the interpolation moments matrix is given. In Section II, the matrix is analyzed in detail. The results of the analysis are presented in Section III a bursting dam example.

A. Spatial Discretization Principle

The postulated adaptivity criterion is based on the principle of spatial discretization. Partial time- and space-dependent differential equations can be spatially discretized and thus transferred into purely time-dependent ordinary differential equations. Thus, the evaluation of a continuous function $A(\mathbf{r}_a)$ and its gradient $\nabla_a A(\mathbf{r}_a)$ at the position \mathbf{r}_a of the reference particle a can be determined by the sum over all neighboring particles b using

$$A(\mathbf{r}_a) = \sum_{b \in B} \frac{m_b}{\rho_b} A(\mathbf{r}_b) W_{ab}, \quad (1)$$

and

$$\nabla_a A(\mathbf{r}_a) = \sum_{b \in B} \frac{m_b}{\rho_b} A(\mathbf{r}_b) \nabla_a W_{ab} \quad (2)$$

with the kernel function $W_{ab} := W(\mathbf{r}_{ab}, h)$, the mass m_b and the density ρ_b of b .

B. SPH Interpolation Moments Matrix

Reducing the number of particles is an option when intending to reduce the calculation effort. A reduction in the number of SPH particles can result in a reduction in spatial interpolation quality. These two factors conflict with each other. As a compromise, the local particle resolution can be adapted dynamically during the simulation. The adaptivity process can generally be divided into the following three steps:

- 1) Identifying regions, where the resolution needs to be adapted.
- 2) Inserting the new SPH particles and determining their state variables.
- 3) Deleting the original SPH particles.

The application of such local adaptive discretization schemes depends usually on position-based criteria or physical criteria. These criteria must be defined prior to the simulation process.

The approach from [2] tries to circumvent this by using the SPH interpolation moments matrix [4]. The SPH interpolation moments matrix can be defined by the residuals resulting from the differences between the exact and the approximate solution for the Taylor series expansion of the two functions $A(\mathbf{r}_a)$ and $\nabla A(\mathbf{r}_a)$ seen in Eq. (1) and Eq. (2). The SPH interpolation moments matrix is

$$\mathbf{M}_a := \sum_{b \in B} \frac{m_b}{\rho_b} \otimes \begin{bmatrix} W_{ab} & -\mathbf{r}_{ab}^x W_{ab} & -\mathbf{r}_{ab}^y W_{ab} & -\mathbf{r}_{ab}^z W_{ab} \\ \partial_a^x W_{ab} & -\mathbf{r}_{ab}^x \partial_a^x W_{ab} & -\mathbf{r}_{ab}^y \partial_a^x W_{ab} & -\mathbf{r}_{ab}^z \partial_a^x W_{ab} \\ \partial_a^y W_{ab} & -\mathbf{r}_{ab}^x \partial_a^y W_{ab} & -\mathbf{r}_{ab}^y \partial_a^y W_{ab} & -\mathbf{r}_{ab}^z \partial_a^y W_{ab} \\ \partial_a^z W_{ab} & -\mathbf{r}_{ab}^x \partial_a^z W_{ab} & -\mathbf{r}_{ab}^y \partial_a^z W_{ab} & -\mathbf{r}_{ab}^z \partial_a^z W_{ab} \end{bmatrix} \stackrel{!}{=} \mathbf{I}. \quad (3)$$

With the distance vector $\mathbf{r}_{ab} := \mathbf{r}_a - \mathbf{r}_b$. It should be noted that the right-hand side corresponds to the identity matrix which represents the ideal shape of the matrix. A deviation of the optimal matrix \mathbf{M}_a can arising from

- the spatial resolution of the model area,
- an irregular distribution of SPH particles, and
- truncated kernel-support at free surfaces [5].

The local error

$$\varepsilon_a = |\det(\mathbf{M}_a) - 1| \quad (4)$$

should be zero and is used as an approach to find areas to refine [2]. This is valid if all interpolation points – based on the reference position \mathbf{r}_a – are symmetrically arranged and the kernel is not truncated. The matrix \mathbf{M}_a is analyzed in this paper to show its changes of the spatial resolution or the particle arrangement. The results of the analysis are presented in this paper.

II. ANALYSIS

Since the yet available adaptivity criteria are position-based or based on physical values, prior knowledge about the system and its behavior is essential. Since this knowledge is not always present, it would be advantageous to automatically identify particles during the runtime of the simulation. One approach is the use of the SPH interpolation moments matrix \mathbf{M}_a in Eq. (3) and its deviation from the identity matrix [5]. An analysis of the matrix \mathbf{M}_a is made in this section.

A. Influences on the SPH Interpolation Moments Matrix

The relationship $\mathbf{M}_a \stackrel{!}{=} \mathbf{I}$ in Eq. (3) represents the ideal case of perfectly arranged and distributed particles. If the particles deviate from this ideal case, the SPH interpolation moments matrix \mathbf{M}_a with $\mathbf{M}_a \neq \mathbf{I}$.

For a more detailed understanding of the matrix and how changes in the particle arrangement affect it, the error sources having an influence on the matrix \mathbf{M}_a must be identified. The influences mentioned in Section I-B are described in more detail below. In [6]–[8] the influences could be classified into the following three error sources.

1) *Spatial Resolution of the Model Domain*: In the context of SPH, spatial resolution is the ratio between the number of SPH particles in the kernel support area to the kernel size. A pure adjustment of the smoothing length h or the ratio $\|\mathbf{r}_a - \mathbf{r}_b\|_2/h$ does not necessarily lead to an improvement but can even lead to a deterioration [6].

2) *Non-Uniformity of the Particle Distribution*: When the distribution of neighbors of a particle is analyzed, their relative positions have a great influence on the entries of the matrix \mathbf{M}_a . Symmetric particle arrangements usually lead to a reduced deviation of the matrix \mathbf{M}_a from the identity matrix.

3) *Free Surfaces*: Free surfaces are defined by particles having a truncated kernel-support. In order to detect free surfaces, it is necessary to identify areas with no particles.

The influences of a non-uniformity of the particle distribution and the truncated kernel-support at free surfaces cannot be completely separated due to their related nature. This leads to a mixture of influences when examining the matrix \mathbf{M}_a . It is now necessary to relate these error source to the provoked deviations in the matrix \mathbf{M}_a from the identity matrix.

B. Procedure

Initial, various grid arrangements are checked and related to the changes in the SPH interpolation moments matrix \mathbf{M}_a entries. In addition to the described matrix \mathbf{M}_a (see Section I-B), also other output values are calculated which are needed for the analysis of the influences on the system as well as the matrix \mathbf{M}_a . Helpful values are the norm of the summed particle distances $\|\Sigma \mathbf{r}_{ab}\|_2$ and the number of neighboring particles N_h . These two values are described in detail in Section II-D.

To analyze the single entries of the matrix \mathbf{M}_a , a homogeneous, Cartesian grid is first chosen. The grid is further modified in such a way that the influences mentioned in Section II-A are provoked. To assess the influence of the non-uniform particle distribution on the matrix \mathbf{M}_a the particles are randomly arranged. Just the minimum distance between particles is specified prior in order to prevent very small particle distances. For the first analysis of the system, this procedure is necessary to provide an overview of the matrix.

To check the influence of a non-uniformity of the particle distribution in more detail particles are removed or added in the analyzed grids. Furthermore, the existing particles are rearranged in order to achieve an irregular particle distribution. For this purpose, the change in the matrix is compared with the initial situation. The results of this preliminary examination are used in the following to analyze the equations of the matrix \mathbf{M}_a . The matrix \mathbf{M}_a is analyzed in the context of an ideal particle grid and other particle patterns.

The found relationships are to be verified first in MATLAB [9] with homogeneous grids and few particles, and then verified by simulating the commonly used bursting dam problem with the software Pasimodo [10].

C. Analysis of the SPH Interpolation Moments Matrix Entries

How the influences mentioned in Section II-A affect the entries of the matrix M_a requires knowledge about the behavior of the entries in the event of changes of different variables. For the analysis, the well-known Wendland C^2 kernel [11] is first used. The kernel can be represented by

$$W_{WC^2}(\zeta_{ab}, h) := \begin{cases} \frac{\alpha_d}{h^d} (1 - \zeta_{ab})^4 (1 + 4\zeta_{ab}) & \text{if } 0 \leq \zeta_{ab} < 1 \\ 0 & \text{else.} \end{cases} \quad (5)$$

With the smoothing length h and the normalized distance $\zeta = \frac{\|\mathbf{r}_{ab}\|_2}{h}$. The gradient of this kernel is expressed as

$$\nabla_a W_{WC^2}(\zeta_{ab}, h) := \begin{cases} \frac{\alpha_d}{h^{d+1}} \frac{\mathbf{r}_{ab}}{\|\mathbf{r}_{ab}\|_2} (-20\zeta_{ab}(1 - \zeta_{ab})^3) & \text{if } 0 \leq \zeta_{ab} < 1 \\ 0 & \text{else.} \end{cases} \quad (6)$$

The constant α depends on the dimension d and takes the value $7/\pi$ for the two-dimensional case and $21/2\pi$ for the three-dimensional case. This kernel is used to build the SPH interpolation moments matrix M_a . In order to better understand it, the entries of the matrix are initially divided into constants and parameters to break down the individual variables to a manageable level. The constant part contains all terms kept constant during the simulation, i. e. the mass m , the kernel pre-factor α , and the density ρ . While the parameters' part contains the kernel in its form, without the fraction $\frac{\alpha}{h}$ and the other variables that changes over the simulation, the variable part depends only on the parameters \mathbf{r}_{ab} and h since $\zeta = \|\mathbf{r}_{ab}\|_2/h$. So, the parameters part contains \mathbf{r}_{ab} and h . All matrix entries can be divided into these two parts. This classification is important for the analysis of the matrix since no constants-part can be excluded by the summation over a particle and its neighboring particles. This makes the matrix more understandable.

For the sake of simplicity, both the mass m and the density ρ specifies as constants and they are not adjusted if the parameters part is changed. Based on this, the constants part remains constant during the simulation. If adjustments are made in terms of particle refinement or coarsening, the constants part would not be constant anymore.

The kernel and its gradient depend purely on ζ , and, thus only on the Euclidean norm of the distance to the neighboring particles $\|\mathbf{r}_{ab}\|_2$ and the smoothing length h . The smoothing length is initially assumed to be identical for all particles. So, the value $\frac{1}{h^d}$ does not change over the summation of the variables. Due to this fact, the smoothing length h of the particles can be considered as constant as well.

If the two parts – constants and parameters – are multiplied and summed-up over all neighboring particles B they result in the matrix M_a entries in Eq. (3).

Therefore, $\|\mathbf{r}_{ab}\|_2$ is the parameter to be considered. According to this, only the distance vector \mathbf{r}_{ab} and its Euclidean norm $\|\mathbf{r}_{ab}\|_2$ are changed for the analysis.

D. Other Parameters

It is the aim of additional values to separate the different influences of Section II-A as far as possible. However, since a distinction has turned out to be difficult in principle, an attempt should be made with additional values to separate the influences. The matrix M_a entries alone do not allow such a consideration due to the correlation. For this analysis, the parameter \mathbf{r}_{ab} has the only impact on the matrix M_a entries. So, it might be useful to check this parameter on its own. The parameter \mathbf{r}_{ab} leads to the two further parameters particle distances and number of neighbors used for the further analysis as well.

1) *Particle Distances*: The norm of the particle distance to the neighboring particles, is included in the calculation of the SPH interpolation moments matrix M_a as $\|\mathbf{r}_{ab}\|_2$. As a further point of the analysis, this norm is summed-up as a separate value. It is described by $\|\Sigma\mathbf{r}_{ab}\|_2$. All distance vectors of the particles – located in the kernel support domain – are summed-up and the Euclidean norm is then taken. Influences of the particle position are to be determined with $\|\Sigma\mathbf{r}_{ab}\|_2$. In the case that the particles are arranged symmetrically around the reference particle, $\|\Sigma\mathbf{r}_{ab}\|_2$ vanishes. If particles are missing or if they are not arranged symmetrically regarding the reference position, this results in $\|\Sigma\mathbf{r}_{ab}\|_2 \neq 0$.

In this way, free surfaces, and asymmetry in the particle arrangement can be determined globally. However, clear distinction between both is not possible using this value alone.

2) *Number of Neighbors*: The number of neighbors is also relevant for the SPH interpolation moments matrix M_a . For this work, the value is described by N_h . The h subscript is chosen because it shows in which area the number N is distributed. Since particles with $\|\mathbf{r}_{ab}\|_2 > h$ have no influence on the matrix M_a due to the conditions given in Eqs. (5) and (6) they are also not counted here. If this value is smaller than an average value, conclusions can be drawn about the resolution or the particle arrangement around this particle.

A sharp distinction from the influences described in Section II-A is not possible, since a small number of particles in the kernel support area could be caused not only by an insufficient resolution but also by free surfaces. However, this value can still serve as an indicator of such influences.

Since the two values $\|\Sigma\mathbf{r}_{ab}\|_2$ and N_h provide information that is related to the matrix M_a , a representation of the matrix M_a versus $\|\Sigma\mathbf{r}_{ab}\|_2$ and N_h can generate useful information about the course of the two values.

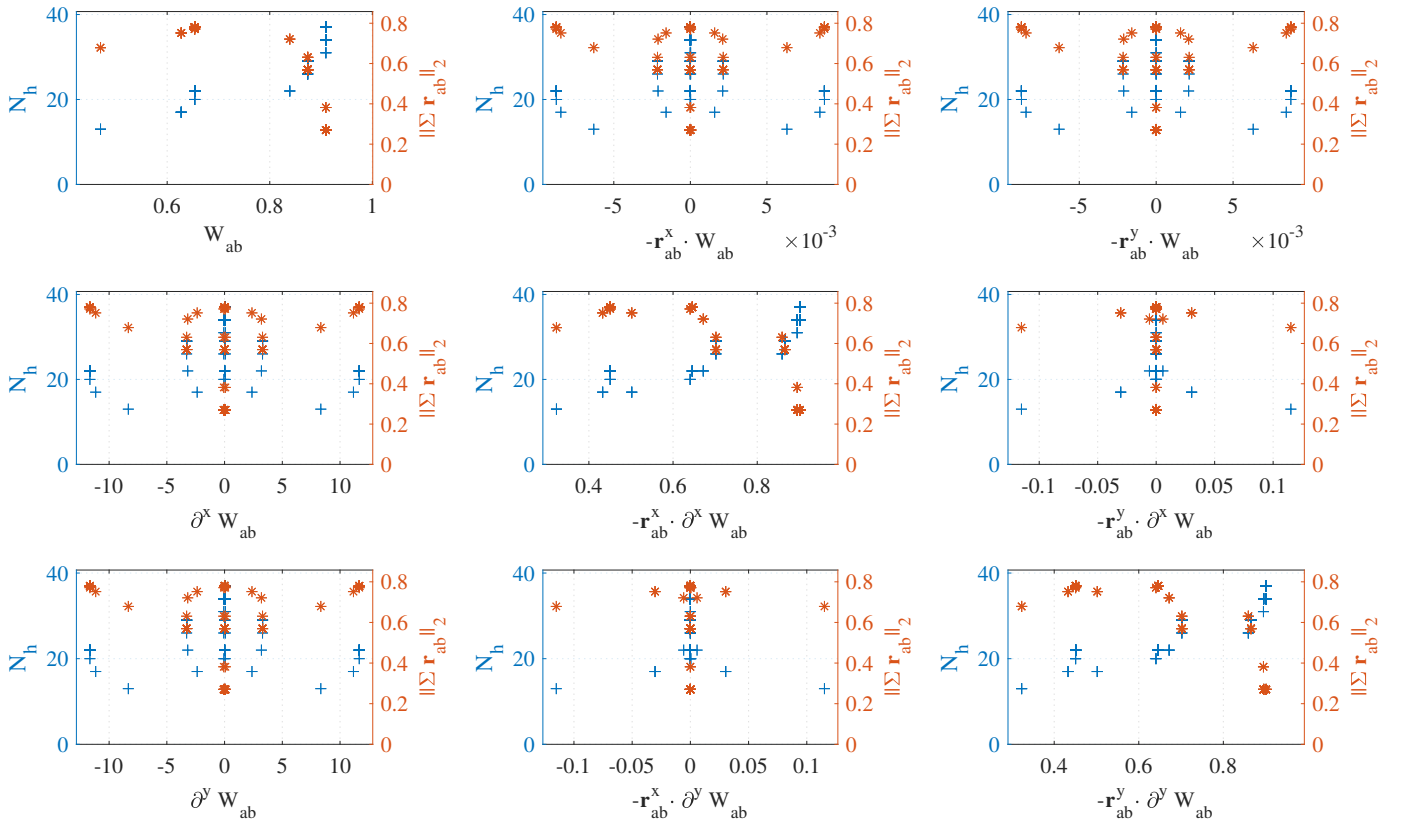


Fig. 1. The number of neighbors N_h (plus) and the norm of summed-up particles distances $\|\Sigma \mathbf{r}_{ab}\|_2$ (asterisk) versus the entries of M_a .

E. Visualization of the SPH Interpolation Moments Matrix

To visualize the SPH interpolation moments matrix M_a , the entries are plotted versus both the total norm of the particle's distances $\|\Sigma \mathbf{r}_{ab}\|_2$ and the number of neighbors N_h . This representation attempts to visualize the course of the matrix M_a in relation to $\|\Sigma \mathbf{r}_{ab}\|_2$ and N_h . The subplots of Fig. 1 are distributed in the same way as the matrix M_a in Eq. (3) for the two-dimensional case in the x - and y -direction.

F. Visualization of the Grid Areas

The SPH interpolation moments matrix M_a has different values at different points on the grid. This behavior is described in more detail below. As it has already been shown, particles that deviate by the influences (see Section II-A) can be found with the matrix M_a . In Fig. 1 the matrix M_a is plotted versus $\|\Sigma \mathbf{r}_{ab}\|_2$ and N_h and shows the course of these deviations.

In Fig. 2 the colors of the left plot show the accumulation of particles with the same position in the right plot, so certain areas of the grid can be assigned to this position. This accumulated representation is also carried out with the subplots from Fig. 1 in order to be able to assign the areas to the matrix M_a entries as well.

Plotting $\|\Sigma \mathbf{r}_{ab}\|_2$ versus N_h shows the other calculated values, which does not require the calculation of the matrix M_a . This representation and both values can also be used to draw

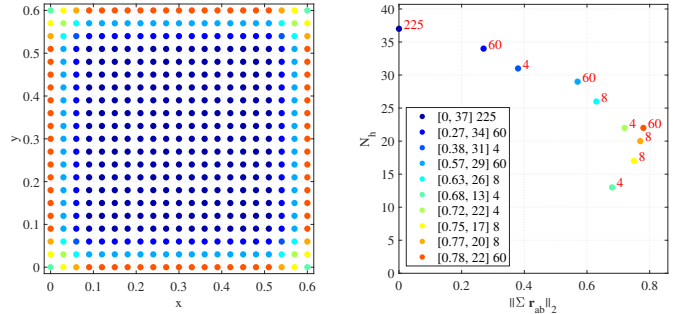


Fig. 2. Visualization of the grid (left) in relation to N_h versus $\|\Sigma \mathbf{r}_{ab}\|_2$ (right).

conclusions about the influences mentioned in Section II-A. The distribution of $\|\Sigma \mathbf{r}_{ab}\|_2$ and N_h for a homogeneous grid is presented in Fig. 2.

This method of representation is chosen to visualize the influences by rearranging the particles. The effects of the free surfaces should also be evaluated by this representation as well.

The mentioned considerations are made under the premise that with changes of the parameters part (see Section II-C) the values mass m and density ρ do not change. This premise is taken due to the fact that the changes only affect individual particles and not entire areas. Rearranging entire areas – for

particle refinement or coarsening – can lead to a change in the density and this is not part of this analysis.

III. RESULTS

This section is based on two aspects. On the one hand, the symmetries of the off-diagonal elements are used to simplify the calculation and, that way, reduce the calculation effort of the matrix M_a . In this context, an attempt is made to find the root of that symmetry and whether these relationships only apply to the Wendland C^2 kernel or if they can generally be found in kernels with a similar course. On the other hand, the connections between the influences on the matrix M_a and the analyzed values are used to formulate an adaptivity criterion for the particle detection during refinement processes.

In Section III-A, the symmetrical relationship of the subplots seen in Fig. 1 are described in more detail. After that, in Section III-B an attempt is made to describe the symmetrical relationship.

The error-detecting values, the implementation of an adaptivity criteria is described and verified with an example in Section III-D. In Section III-D, the implemented adaptivity criterion is also used to verify the symmetric relationships between the off-diagonal elements of the matrix M_a .

A. Off-Diagonal Elements

The representation of the matrix M_a entries seen in Fig. 1 shows an interesting behavior of the off-diagonal elements. It could be observed that the off-diagonal elements appear mirrored at the main diagonal. On closer inspection it was noted that, although the entries are similar in distribution, they are scaled differently. So, there seems to be a linear relationship between these SPH interpolation moments matrix M_a entries and to verify this, the elements $-\mathbf{r}_{ab}^x W_{ab}$ have been plotted versus $\partial_a^x W_{ab}$. First for a homogeneous grid, then also for a random grid. Figure 3 shows the two values $\nabla_a W_{ab}$ and $\mathbf{r}_{ab} W_{ab}$ for the x -related parts of the matrix M_a . A linear correlation is recognizable in this mode of representation and is further illustrated by the diagonal of the linear fitting function. However, it can also be seen that there are also deviations around the fitting function. This topic is covered in Section III-B. Figure 3 is representative for all off-diagonal elements. Note that the submatrix of the matrix M_a described by

$$M_{a, \text{first}} := \sum_{b \in B} \frac{m_b}{\rho_b} \mathbf{r}_{ab} \nabla_a W_{ab} \quad (7)$$

$$M_{a, \text{first}} := \sum_{b \in B} \frac{m_b}{\rho_b} \begin{pmatrix} -\mathbf{r}_{ab}^x \partial_a^x W_{ab} & -\mathbf{r}_{ab}^y \partial_a^x W_{ab} & -\mathbf{r}_{ab}^z \partial_a^x W_{ab} \\ -\mathbf{r}_{ab}^x \partial_a^y W_{ab} & -\mathbf{r}_{ab}^y \partial_a^y W_{ab} & -\mathbf{r}_{ab}^z \partial_a^y W_{ab} \\ -\mathbf{r}_{ab}^x \partial_a^z W_{ab} & -\mathbf{r}_{ab}^y \partial_a^z W_{ab} & -\mathbf{r}_{ab}^z \partial_a^z W_{ab} \end{pmatrix} \stackrel{!}{=} \mathbf{I}, \quad (8)$$

is symmetric. In Eq. (8) the matrix M_a of Eq. (3) is shown without the first row and column.

The established relationships now raise the question of whether the values of the matrix M_a can also be calculated with the kernel W_{ab} and the distance vector \mathbf{r}_{ab} . So, if the

matrix M_a is sufficiently described replacing the gradient ∇W_{ab} with

$$\nabla W_{ab} \approx -\mathbf{r}_{ab} W_{ab}, \quad (9)$$

or written in index notation as

$$\partial_a^x W_{ab} \approx -\mathbf{r}_{ab}^x W_{ab} \quad (10)$$

$$\partial_a^y W_{ab} \approx -\mathbf{r}_{ab}^y W_{ab} \quad (11)$$

$$\partial_a^z W_{ab} \approx -\mathbf{r}_{ab}^z W_{ab}. \quad (12)$$

Then the matrix M_a can be represented as

$$M_{a, \text{con}} := \sum_{b \in B} \frac{m_b}{\rho_b} W_{ab} \otimes \begin{pmatrix} 1 & -\mathbf{r}_{ab}^x & -\mathbf{r}_{ab}^y & -\mathbf{r}_{ab}^z \\ -\mathbf{r}_{ab}^x & \mathbf{r}_{ab}^{x^2} & \mathbf{r}_{ab}^y \mathbf{r}_{ab}^x & \mathbf{r}_{ab}^z \mathbf{r}_{ab}^x \\ -\mathbf{r}_{ab}^y & \mathbf{r}_{ab}^x \mathbf{r}_{ab}^y & \mathbf{r}_{ab}^{y^2} & \mathbf{r}_{ab}^z \mathbf{r}_{ab}^y \\ -\mathbf{r}_{ab}^z & \mathbf{r}_{ab}^x \mathbf{r}_{ab}^z & \mathbf{r}_{ab}^y \mathbf{r}_{ab}^z & \mathbf{r}_{ab}^{z^2} \end{pmatrix} \stackrel{!}{=} \mathbf{I}. \quad (13)$$

For the homogeneous Cartesian particle grid described here, the similarities are recognizable as shown in the Eq. (13). The same behavior can also be observed for a random particle arrangement. Based on this, a general connection between these entries can be concluded. The reformulation of the matrix M_a leads to a reduction in the calculation effort.

The connection was found using the Wendland kernel. To check whether the behavior also occurs with the

- Wendland C^2 ,
- Poly 6 [12],
- Wendland C^4 [11],
- Gaussian [13], and
- Cubic Spline [13]

kernels, they have been analyzed like it is described in Section II. These kernels share similar courses, which suggests that the behavior observed is the same. The described relationship has not been generally proven. Only for the specified kernels the same behavior was found. To draw a general conclusion – from kernels with the same structure – further research is required and necessary.

B. Root of the Connections

To explain the relationship of Eq. (9), the functions for the Wendland C^2 kernel W_{ab} and its gradient divided by the position vector $\mathbf{r}_{ab}^{-1} W_{ab}$ are plotted versus the Euclidean norm $\|\mathbf{r}_{ab}\|_2$ (see Fig. 4). It is multiplied by the transpose position vector because it represents only one factor for the matrix entries and the relationship can be recognized even without it. The kernel is dependent on $\|\mathbf{r}_{ab}\|_2$ and no longer of h , since h is assumed to be constant for the consideration and in the analyzed cases. The upper bound of $\|\mathbf{r}_{ab}\|_2$ can thus be represented by $\|\mathbf{r}_{ab}\|_2 = h$. A consideration of values $\|\mathbf{r}_{ab}\|_2 > h$ does not make sense here. Figure 4 illustrates the course and the relationship of the mentioned Eq. (9). Note that this plot is the course of only one particle pair. For the calculation of the matrix M_a , these values are summed-up as described in Eq. (3).

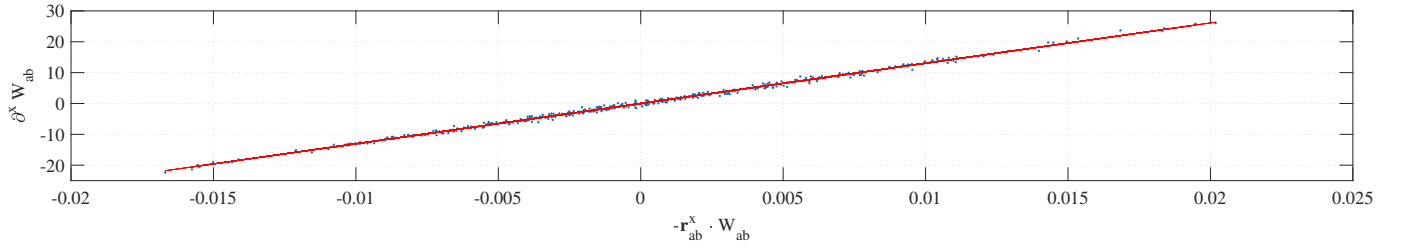


Fig. 3. Visualization of the off-diagonal elements $\partial_a^x W_{ab}$ versus $\mathbf{r}_{ab}^x \cdot W_{ab}$ for random distributed particles arrangements

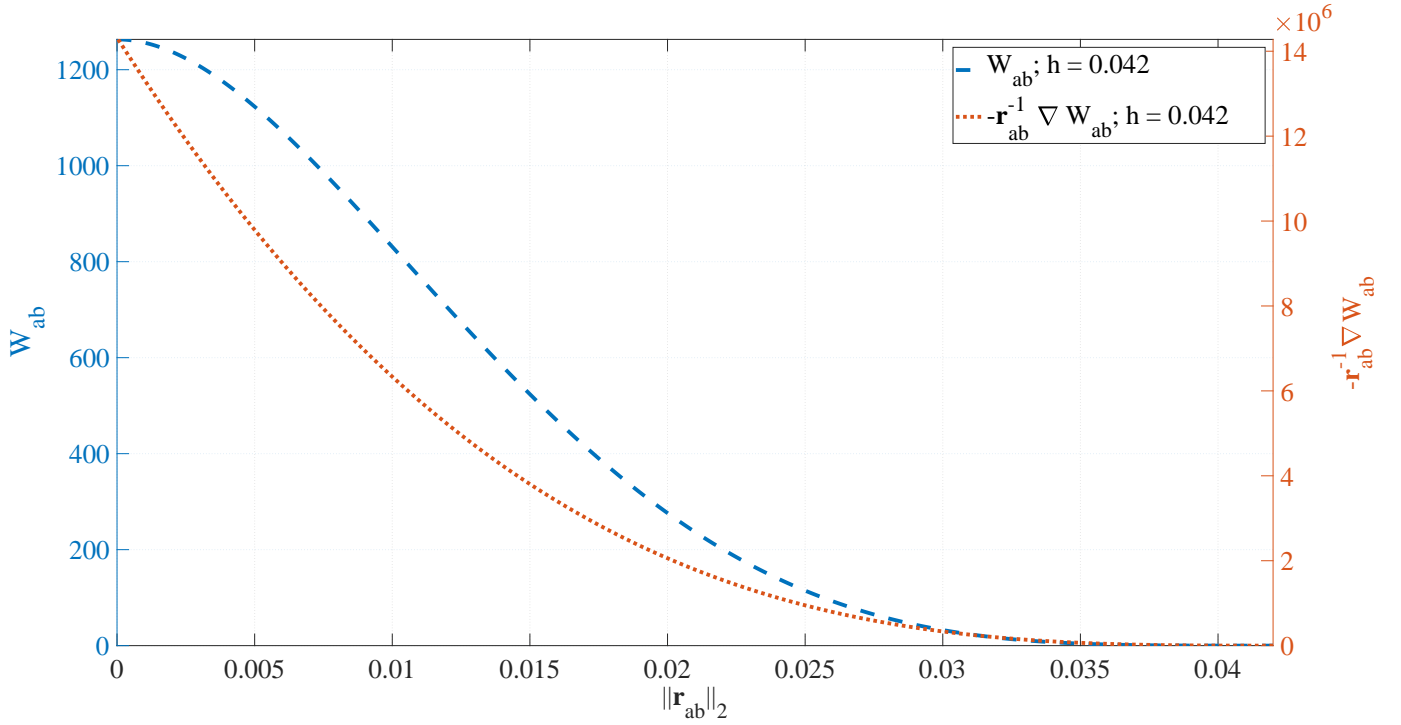


Fig. 4. SPH Interpolation moments matrix entries W_{ab} and their derivatives ∇W_{ab} multiplied by \mathbf{r}_{ab}^{-1} with a constant smoothing length versus $\|\mathbf{r}_{ab}\|_2$.

The shown relationship or the deviation of the functions coincides with the observations from Fig. 4. There, deviations around a constant effective value are found. For example, the gradient could be approximated as

$$\frac{d}{d\mathbf{r}} W(\mathbf{r}) = \mathbf{r}^{-5}. \quad (14)$$

The antiderivative of this equation would be

$$W(\mathbf{r}) = -\frac{1}{4}\mathbf{r}^{-4} = -\frac{1}{4}\mathbf{r} \frac{d}{d\mathbf{r}} W(\mathbf{r}). \quad (15)$$

If this is compared with the matrix \mathbf{M}_a , the parallels can be recognized. A scaling factor and the derivative (gradient) can also be seen here.

C. Error-Detecting Values

Based on the found connections between the SPH interpolation moments matrix \mathbf{M}_a and the other variables $\|\Sigma \mathbf{r}_{ab}\|_2$ and N_h (see Section II-D), an attempt is made to separate the influences described in Section II-A. The background

of the analysis of the matrix \mathbf{M}_a is the introduction of an adaptivity criterion, as already started in [1], [2], and [3]. Such a criterion should make it possible during the runtime of the simulation to automatically detect areas which are suitable for particle refinement or coarsening. This should be done using this matrix. An analysis and the behavior of the matrix \mathbf{M}_a is therefore of significant importance. Through the shown relationships and modes of representation, it seems that the complete matrix is not relevant for such a criterion and other variables $\|\Sigma \mathbf{r}_{ab}\|_2$ and N_h deliver information for the particle refinement or coarsening as well.

Based on these correlations, an adaptivity criterion could be based on the values for

- the kernel function W_{ab} ,
- its gradient ∇W_{ab} ,
- the positions of the particles \mathbf{r}_{ab} ,
- the sum of the Euclidean norm $\|\Sigma \mathbf{r}_{ab}\|_2$, and
- the number of neighbors N_h .

In the following section, a first attempt to implement such

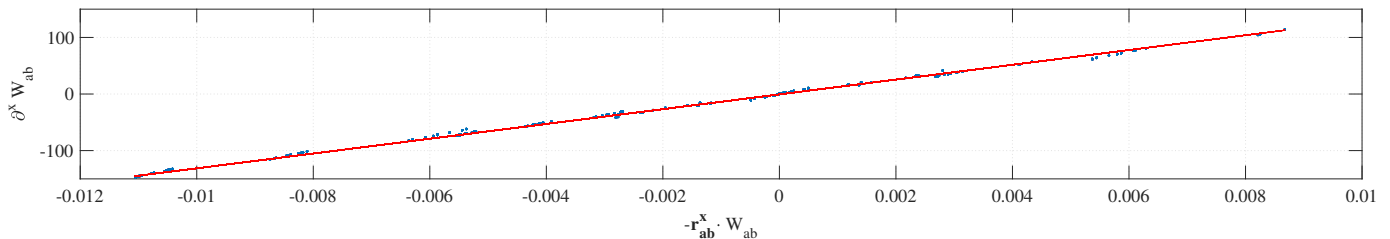


Fig. 5. Representing the off-diagonal elements $\partial_a^x W_{ab}$ versus $r_{ab}^x W_{ab}$ for the bursting dam example.

a criterion in the SPH simulation software Pasimodo [10] is described.

D. Adaptivity Criterion and Example

To formulate an adaptivity criterion and check the symmetric relationships between the off-diagonal elements, the SPH interpolation moments matrix M_a is implemented in the software Pasimodo. These data are first used to check the relationship $\nabla W_{ab} = -r_{ab} W_{ab}$. To verify this connection, a bursting dam problem is used.

A linearity of the two values, representative for the other off-diagonal elements, seen in Fig. 3 can also be seen for the output $\partial_a^x W_{ab}$ and $r_{ab}^x W_{ab}$ calculated for the bursting dam problem, and is shown in Fig. 5. With this knowledge, the calculations cost can be reduced, since not all entries of the matrix M_a are required for detection of influences described in Section II-A).

For an adaptivity criterion, in a first step, the calculation of the matrix M_a and the other parameters $\|\Sigma r_{ab}\|_2$ and N_h , must be carried out for each particle and each time step. In a second step, average values can be calculated and compared to the values of specific particles.

The analysis of the matrix M_a enabled to find the described correlations of the matrix M_a entries and the influences of a low spatial resolution as well as a non-uniformity of the particle distribution using the additional other parameters norm of the summed particle distances $\|\Sigma r_{ab}\|_2$ and the number of neighboring particles N_h .

With the help of the diagonal elements of the Matrix M_a and the summed-up distances $\|\Sigma r_{ab}\|_2$, the first results for the categorization of refinement areas could already be achieved. For the classification, the matrix M_a for each particle is compared with the average of the respective value and divided into two categories. The particles with a high deviation – in relation to the average – are used for the classification of the areas.

Since the matrix M_a of edge particles already have a larger deviation from the identity matrix due to the free surface, these particles must not be considered in the classification. The analysis of the matrix has shown that the diagonal elements, which take the distance into account, are suitable for detecting edge particles. On the one hand, the first diagonal element provides poorer results for this, but on the other hand this element is suitable for recognizing a low spatial resolution. For

detection of areas with poor resolution, edge particles found are no longer taken into account.

In Fig. 6 a two-dimensional bursting dam example can be seen. It also shows the particles marked by the described adaptivity criterion that are going to be refined. The initial particles setup and parameters are based on the problem dealt with in [14]. The boundaries are considered by a free-slip condition according to [15].

IV. CONCLUSION

In this paper, a fundamental analysis of the SPH interpolation moments matrix M_a was carried out. First, the theoretical background of this matrix M_a was introduced. In a nutshell, the required foundation of equations and specifications for the consideration was laid out.

In the next step, the matrix was thoroughly analyzed with the help of this foundation. First, the influences to be considered were determined. The aim was to derive the influences based on the matrix M_a and to separate them sharply from one another. Since a clear distinction based on the pure matrix M_a entries is not possible, additional values were needed for this purpose, which should make such a differentiation easier. With help of this additional information, an exact distinction is not yet possible, but can still be used in practice, which was also shown.

Another connection that emerged during the analysis is an indicated symmetry of the off-diagonal elements (Section III-A). In the case of a non-refined or coarsened simulation, the off-diagonal elements behave symmetrically and can thus be broken down to a simpler representation – considering the calculation effort (Section III-A). One possible reason this relationship could come from is the similarity of the kernel multiplied by the position $-r_{ab}$ and the gradient ∇W_{ab} (Section III-B). Functions with such a course could generally feature this relationship. To check these relationship, the matrix M_a was implemented in the SPH simulation software Pasimodo and checked with the calculated data (Section III-D). The relations between the off-diagonal elements of the matrix M_a were also observed in other commonly used kernels (see Section III-A) but could not be proven generally. Further considerations are still necessary.

With help of the knowledge brought by the analyzes, an adaptivity criterion could now be introduced. The first approaches for this have already been implemented in Pasimodo and are also delivering useful results. The adaptivity criterion

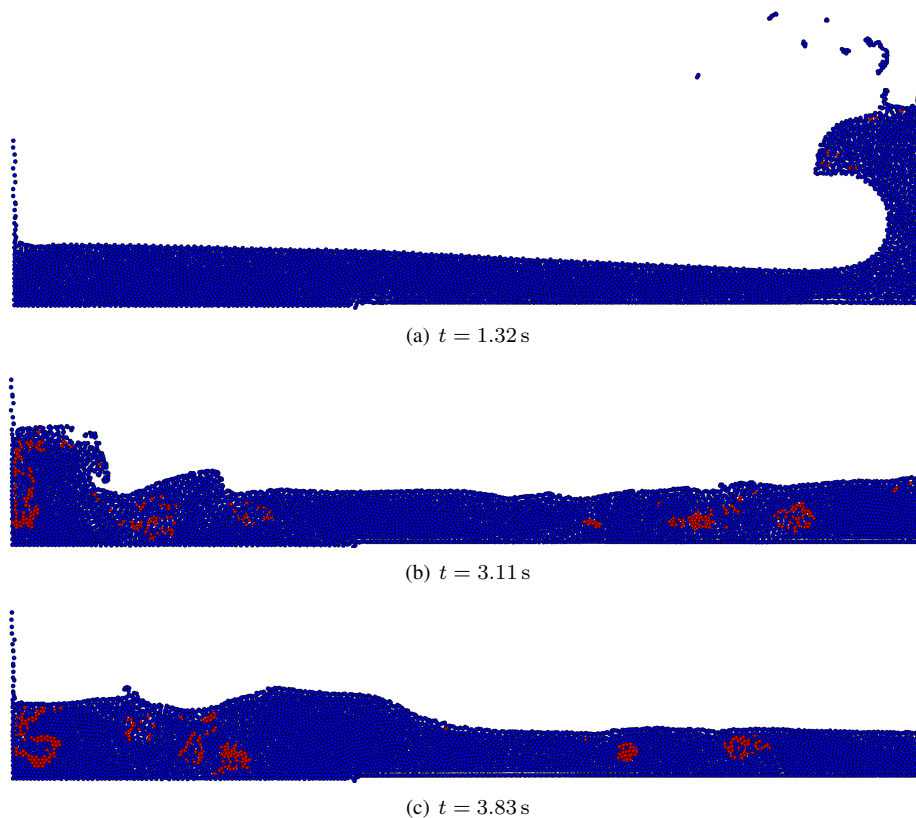


Fig. 6. Bursting dam example showing particles marked for refinement.

can now be further expanded and adapted. In the context of further research concerning this topic, other kernels, and a general relation between the matrix M_a entries mentioned in Section III-B should be investigated in detail. Edge particles or free surfaces could also be detected with the aid of the matrix M_a . Furthermore, a consideration of the influences of the other variables, e.g. the smoothing length, could be useful. An analysis of the matrix after particle refinement or coarsening should provide additional insights for further work.

REFERENCES

- [1] F. Spreng and P. Eberhard, "An approach to error-estimation-based adaptivity in smoothed particle hydrodynamics," *Proceedings of the 10th International SPHERIC Workshop*, pp. 155–162, 2015.
- [2] F. Spreng, P. Eberhard, and R. Vacondio, "A novel, purely methodological strategy for controlling dynamic resolution in smoothed particle hydrodynamics," *Proceedings of the 11th International SPHERIC Workshop*, pp. 31–38, 2016.
- [3] F. Spreng, J. R. Williams, R. Vacondio, and P. Eberhard, "An adaptivity criterion for smoothed particle hydrodynamics fluid simulations based on spatial discretization error," *Proceedings of the 12th International SPHERIC Workshop*, pp. 338–345, 2017.
- [4] G. Fourtakas, R. Vacondio, and B. D. Rogers, "On the approximate zeroth and first-order consistency in the presence of 2-d irregular boundaries in sph obtained by the virtual boundary particle methods," *International Journal for Numerical Methods in Fluids*, vol. 78, no. 8, pp. 475–501, 2015.
- [5] F. Spreng, R. Vacondio, P. Eberhard, and J. R. Williams, "An advanced study on discretization-error-based adaptivity in smoothed particle hydrodynamics," *Computers & Fluids*, vol. 198, p. 104388, 2020.
- [6] N. J. Quinlan, M. Basa, and M. Lastiwka, "Truncation error in mesh-free particle methods," *International Journal for Numerical Methods in Engineering*, vol. 66, no. 13, pp. 2064–2085, 2006.
- [7] A. Amicarelli, J.-C. Marongiu, F. Leboeuf, J. Leduc, M. Neuhauser, Le Fang, and J. Caro, "Sph truncation error in estimating a 3d derivative," *International Journal for Numerical Methods in Engineering*, vol. 87, no. 7, pp. 677–700, 2011.
- [8] L. Di G. Sigalotti, J. Klapp, O. Rendón, C. A. Vargas, and F. Peña-Polo, "On the kernel and particle consistency in smoothed particle hydrodynamics," *Applied Numerical Mathematics*, vol. 108, pp. 242–255, 2016.
- [9] The MathWorks, Inc. (17.04.2021) Mathworks – entwickler von matlab und simulink. [Online]. Available: <https://de.mathworks.com/>
- [10] Pasimodo. (01.04.2021) Pasimodo: Pasimodo is a program package for particle-based simulation methods. [Online]. Available: <https://www.itm.uni-stuttgart.de/en/software/pasimodo>
- [11] H. Wendland, "Piecewise polynomial, positive definite and compactly supported radial functions of minimal degree," *Advances in Computational Mathematics*, vol. 4, no. 1, pp. 389–396, 1995.
- [12] A. Lavrov, P. Skjetne, B. Lund, E. Bjønnes, F. O. Bjørnson, J. O. Busklein, T. Coudert, P. Klebert, K. O. Lye, J. E. Olsen, C. Pákozdi, J. Seland, and W. Yang, "Density-consistent initialization of sph on a regular cartesian grid: Comparative numerical study of 10 smoothing kernels in 1, 2 and 3 dimensions," *Procedia IUTAM*, vol. 18, pp. 85–95, 2015.
- [13] P. J. Cossins, "Smoothed particle hydrodynamics: Or: How i learned to stop worrying and love the lagrangian," Ph.D. dissertation, 2010. [Online]. Available: <http://arxiv.org/pdf/1007.1245v2>
- [14] A. Colagrossi and M. Landrini, "Numerical simulation of interfacial flows by smoothed particle hydrodynamics," *Journal of Computational Physics*, vol. 191, no. 2, pp. 448–475, 2003.
- [15] S. Adami, X. Y. Hu, and N. A. Adams, "A generalized wall boundary condition for smoothed particle hydrodynamics," *Journal of Computational Physics*, vol. 231, no. 21, pp. 7057–7075, 2012.